Journal Pre-proofs

Short communication

Glenohumeral stabilizing roles of the scapulohumeral muscles: Implications of muscle geometry

Daanish M. Mulla, Joanne N. Hodder, Monica R. Maly, James L. Lyons, Peter J. Keir

PII: S0021-9290(19)30852-8
DOI: https://doi.org/10.1016/j.jbiomech.2019.109589
Reference: BM 109589

To appear in: *Journal of Biomechanics*

Received Date: 3 May 2019
Revised Date: 17 December 2019
Accepted Date: 18 December 2019

Please cite this article as: D.M. Mulla, J.N. Hodder, M.R. Maly, J.L. Lyons, P.J. Keir, Glenohumeral stabilizing roles of the scapulohumeral muscles: Implications of muscle geometry, *Journal of Biomechanics* (2019), doi: https://doi.org/10.1016/j.jbiomech.2019.109589

Glenohumeral stabilizing roles of the scapulohumeral muscles: Implications of muscle geometry

Daanish M. Mulla[1], Joanne N. Hodder[2], Monica R. Maly[1,3], James L. Lyons[1], Peter J. Keir[1*]

[1]Department of Kinesiology, McMaster University, Hamilton, ON, Canada
[2]Faculty of Applied Health & Community Studies, Sheridan College, Brampton, ON, Canada
[3]Department of Kinesiology, University of Waterloo, Waterloo, ON, Canada

*Corresponding Author:
Peter J. Keir, PhD
McMaster University
Department of Kinesiology
Ivor Wynne Centre, room 212
1280 Main Street West
Hamilton, ON, Canada, L8S4K1
Telephone: 905-525-9140 ext. 23543
Email: pjkeir@mcmaster.ca

Prepared for submission to: Journal of Biomechanics

Manuscript Type: Short Communication

Word Count: 2070 words

Keywords: Biomechanics, shoulder, probabilistic modeling, upper extremity, joint stability

Abstract

Dynamic stability provided by muscles is integral for function and integrity of the glenohumeral joint. Although the high degree of inter-individual variation that exists in musculoskeletal geometry is associated with shoulder injuries, there is limited research associating the effects of muscle geometry on the potential stabilizing capacities of shoulder muscles. The purpose of this investigation was to evaluate the stabilizing functions of the scapulohumeral muscles using computational modeling and to quantify the sensitivity of muscle stabilizing roles to changes in muscle geometry. Muscle stability ratios in the superior/inferior and anterior/posterior directions were computed as the ratio between the muscle's shear components relative to compression throughout arm elevation in the scapular plane. Muscle attachment locations on the clavicle, scapula, and humerus were iteratively adjusted using Monte Carlo simulations. Consistent with previous experimental studies, the rotator cuff muscles were identified as the primary stabilizers of the glenohumeral joint; whereas the deltoids and coracobrachialis have a strong potential for superiorly translating the humerus at low elevation angles. Variations in the stability ratios due to altered muscle geometry were muscle- and angle-specific. In general, the highest variation was observed for the subscapularis and deltoids (at low elevation angles), while the remaining rotator cuff muscles largely maintained their capacity to provide compressive stabilizing forces at the glenohumeral joint. Changes in muscle stability ratios may affect dynamic stability of the humerus that could differentially predispose individuals to greater risk for injury.

Introduction

The shoulder complex consists of numerous muscles enabling movement across several degrees of freedom unlike any other body part. Enhanced shoulder mobility comes at the expense of glenohumeral (GH) joint stability (Lippitt & Matsen, 1993). Clinically, instability is defined as humeral displacement deemed too large in response to an externally applied force (Veeger & van der Helm, 2007). Excessive humeral translation due to joint instability is common within clinical populations (Poppen & Walker, 1976; Peltz et al. 2015) and can reduce shoulder functionality, cause subluxation/dislocation, and promote mechanical compression of soft tissues leading to subacromial impingement (Michener et al., 2003). GH joint stability is primarily enforced dynamically by muscle forces at mid-ranges of motion. As muscles cause multi-axis translational and rotational accelerations, coordination between muscles requires a delicate balance of forces/moments to facilitate performance while maintaining shoulder complex integrity.

Dynamic stabilizing roles are muscle-specific. The rotator cuff muscles are the primary GH joint stabilizers (e.g. Halder et al., 2001a,b; Lee et al. 2000; Soslowsky et al., 1997). Loading across these muscles enables compression between the convex-shaped humeral head and concave-shaped glenoid. Congruent fit between the two surfaces due to compressive muscle loads is foundational for GH joint stability, referred to as the concavity compression (Lippitt & Matsen, 1993). Stability is maintained as the net joint reaction force is directed within the glenoid arc. In contrast, the deltoids generate greater shear forces, either stabilizing or destabilizing the humerus depending on direction of the externally applied force and shoulder posture (Lee & An, 2002).

Muscle stabilizing potential can be assessed using a ratio between the muscle's shear and compression vector component. Although studies have quantified muscle stability ratios (Ackland & Pandy 2009; Yanagawa et al., 2008), inter-individual differences remain unclear. Wide population-level distributions of bone geometry (Boileau & Walch, 1997; Chopp-Hurley et al., 2016), can theoretically alter muscle lines of action (Hughes et al., 2003; Nyffeler et al., 2006) affecting inter-individual variance in muscle stabilizing functions (Moor et al., 2016), and consequently, muscle synergies required for joint stability. Associations between bone morphology and shoulder injuries (Banas et al., 1995; Hughes et al., 2003; Nyffeler et al., 2006) suggest that altered muscle dynamic stability among individuals may be influenced by bone geometry variations. Using probabilistic modeling, high sensitivity in rotator cuff forces to attachment changes occurs during humeral rotation (Chopp-Hurley et al., 2014); however, the extent to which anatomy affects stabilizing functions for scapulohumeral muscles throughout a range of motion is unknown. The purpose of this study was to predict the range of variation in scapulohumeral muscle stabilization roles due to musculoskeletal geometry changes based on available experimental data.

Methods

The current investigation extends prior analyses examining muscle moment arms and lines of action (Mulla et al., 2019). Scapulohumeral muscle stabilizing roles were investigated using the modified Delft Shoulder and Elbow Model (DSEM) (Blana et al., 2008). Coordinate systems were transformed to match International Society of Biomechanics (ISB) conventions (Wu et al., 2005). A modified Z-axis for the scapular coordinate system was used to represent the glenoid plane when calculating the muscle stability ratios. The Z-axis (glenoid normal

vector) was defined along the vector connecting the glenohumeral joint center (GH) and root of the scapular spine (TS).

Probabilistic modeling quantified stability sensitivity. Univariate normal distributions were generated for coordinates defining 3D muscle attachments at the scapula/clavicle and humerus. Mean values were based on current DSEM with standard deviations from Högfors et al. (1987). Monte Carlo simulations were used to quantify the distribution of model-predicted stability ratios based on muscle attachment perturbations (relative to attached bone's coordinate system). For each muscle element (Table 1), 1000 lines of action were simulated by randomly sampling from the attachment distributions at origin and insertion.

The model was set in static humeral scapular plane elevation angles from 15-120° based on mean data from asymptomatic individuals during dynamic motion (Ludewig et al., 2009). Muscle lines of action, defined in the modified scapular coordinate system, were computed using the unit vector direction cosine. For muscles constrained by wrapping objects, the unit vector was calculated from the origin at the scapula/clavicle and the first contact point on the humerus (i.e. "effective insertion"). Stability ratios quantified each muscle's shear contribution in the superior/inferior (f_y) and anterior/posterior (f_x) directions relative to compression (f_z):

$$ST_{S-I} = \frac{f_y}{|f_z|} \quad (1)$$

$$ST_{A-P} = \frac{f_x}{|f_z|} \quad (2)$$

Where, $ST_{S\text{-}I}$ is the superior/inferior stability ratio, $ST_{A\text{-}P}$ is the anterior/posterior stability ratio, and $f_x/f_y/f_z$ refer to the unit vector direction cosines. Positive $ST_{S\text{-}I}$ and $ST_{A\text{-}P}$ indicate superior

and anterior lines of action, respectively. Stabilizing roles are based on the humeral translations that they prevent (e.g. "superior stabilizers" are muscles with an inferior line of action, preventing superior humeral translation). Stability ratios are based on muscle geometry, independent of force.

Muscle elements were grouped into sub-regions for data reduction (Table 1). Multiple regressions quantified sensitivity of stability ratios to attachment perturbations. The 6 coordinates (XYZ) defining each muscle's attachments at the scapula/clavicle and humerus were included in the regression, along with humeral elevation angle (HT) and its quadratic term (HT^2) to model nonlinearities. To allow comparison across muscles, attachment locations (expressed in the attached bone coordinate system) were centred to the mean and divided by the standard deviation (e.g. □=0.1 interpreted as a 1 standard deviation change in attachment predicts a 0.1 unit change in stability ratio). Regression coefficients were used to evaluate sensitivity of stability ratios to attachment changes. The other predictors within the regression model (HT, HT^2) were not standardized as the comparisons between predictors was focused only on attachment locations and not elevation angle. Interaction terms were not included as they produced minimal changes in model fit. Separate regressions performed at elevation angles of 45°, 90°, and 120° found that stability ratio sensitivities depend on elevation angle for deltoids and coracobrachialis (supplementary material). Thus, models presented represent sensitivity of stability ratios averaged across elevation angles.

**********Table 1 here**********

Results

Superior/Inferior Stability Ratios

Superior/inferior stability ratios are plotted in Figure 1 and summarized in Table 2. The rotator cuff muscles and teres major exhibited small stability ratios (< 1.0), indicating a larger compression vector component than superior/inferior shear. These muscles were superior stabilizers, except for the supraspinatus. The superior sub-regions of the infraspinatus and subscapularis exhibited capacity for either superior or inferior stability, depending on sub-region and attachment locations. The stability ratios for the rotator cuff muscles and teres major were consistent across humeral elevation angle, with divergences at higher elevations (Table 3). In contrast, the deltoids and coracobrachialis exhibited large inferior stabilizing roles that were pronounced at low elevation but decreased non-linearly with increasing elevation. The stabilizing roles of the deltoids were highly sensitive to attachment changes at low elevation, with standard deviations in ST_{S-I} ratio ranging from 0.18-0.47 at 15° elevation. Scapular attachment in the y-axis (superior/inferior) promoted the greatest changes in the superior-inferior stability ratios. A one standard deviation change in scapular attachment along the y-axis predicted changes in stability ratio of at least 0.1 units across most muscles (Table 3). In contrast, one standard deviation perturbation at other coordinates predicted less than 0.05 unit change in the stability ratio for most cases.

**********Table 2 here**********

**********Table 3 here**********

**********Figure 1 here**********

Anterior/Posterior Stability Ratios

Anterior/posterior stability ratios are plotted in Figure 2 and summarized in Table 2. The infraspinatus, supraspinatus, teres minor, coracobrachialis, and anterior deltoid were posterior humeral stabilizers. The subscapularis, teres major, and middle/posterior deltoids were anterior humeral stabilizers. All muscles displayed predominantly small anterior/posterior shear vector components (stability ratios < 1.0). Muscle stability ratios were most sensitive to scapular attachment changes along the x- (anterior/posterior) and z-axes (compression) (Table 4). In contrast, the anterior/posterior stability ratios were robust to changes at other attachment coordinates.

**********Table 4 here**********

**********Figure 2 here**********

Discussion

The current investigation quantified sensitivity of muscle stability ratios to changes in muscle attachments to reflect inter-individual musculoskeletal geometry differences. The rotator cuff muscles act as the primary GH joint stabilizers, while the deltoids and coracobrachialis exhibited substantial superior shear components at low elevation. All muscles displayed small anterior/posterior shear capacities. Perturbations in attachments predicted small to large effects on stability ratios, dependent upon muscle and humeral elevation angle.

Muscle forces are critical for joint stability. Rotator cuff muscle stability ratios were small across all shear directions, reinforcing literature regarding their ability to enforce joint compression. The supraspinatus was predicted to apply a superior shear on the humerus. This finding is consistent with modeling studies (Ameln et al. 2018; Yanagawa et al. 2008) but

contradicts cadaveric studies that measured an inferior directed line of action (Ackland & Pandy, 2009; Graichen et al., 2001; Poppen & Walker, 1978). Differences are small in magnitude and may be due to methodological differences; however, all studies reported a predominantly compression-oriented line of action. A significant contribution of these findings extending the work by Ackland & Pandy (2009) is the analysis of muscle sub-regions. Previous studies commonly grouped muscles into a single line of action. However, shoulder muscles are broad-spanning, having multiple innervation branches and functional sub-regions (Kim et al. 2017; Webb et al., 2014). It should be noted that the muscle elements in the DSEM represent mechanical effects as opposed to anatomical lines of action. Consistent with literature, the deltoids and coracobrachialis display a large superior shear (Halder et al., 2001a; Lee & An, 2002). The superior pull is pronounced at low elevation, corresponding with superior humeral translation during early arm elevation (Bey et al., 2008; Chopp et al., 2010). To visualize the muscle stabilizing functions, stability ratios are plotted together in Figure 3. Included are experimentally determined thresholds (Lippitt & Matsen, 1993) based on the magnitude of net joint reaction forces directed tangentially required to overcome the concavity compression mechanism for stability and dislocate the humeral head. Note that muscle stability ratios do not account for muscle force, which further influences joint stability.

**********Figure 3 here**********

Attachment changes had varying effects on muscle stabilizing function. The supraspinatus, teres minor, and infraspinatus maintained capacity for joint stability despite altered attachments. In contrast, the subscapularis and deltoids had larger deviations in stability

ratios. The net humeral joint reaction force must be directed within a small area on the glenoid face to ensure joint stability. As muscles are an essential component of the net force, muscle forces need to concurrently optimize stability and movement. It is widely acknowledged that inter-individual anatomical differences affect muscle functional roles, but not yet explicitly investigated (Veeger & van der Helm, 2007). Inter-individual musculoskeletal geometry differences affect muscle stabilizing roles, theoretically altering muscle coordination to maintain stability. Increased glenoid inclination and lateral extension of the acromion are correlated with rotator cuff tears (Hughes et al., 2003; Moor et al., 2016). Geometry changes can increase the middle deltoid superior vector component leading to superior humeral instability and increased impingement risk at low elevation angles. Our simulations support this mechanism, with middle deltoid experiencing substantially higher superior stability ratios at 45° elevation when the scapular attachments are perturbed superiorly and laterally (supplementary Table A.1). Compensatory rotator cuff and/or glenohumeral adductor activity would be required to maintain stability (Steenbrink et al., 2009; Gerber et al., 2014; Moor et al., 2016) (Figure 3). Furthermore, as individual musculoskeletal geometry defines spatial relationships between bones and mechanical joint coupling, geometric variation can contribute to the commonly observed inter-individual variation in shoulder kinematics. Overall, understanding individual differences in musculoskeletal geometry and its effect on shoulder function can provide several insights into muscle synergies that can help evaluate how individuals optimize movement and stability, and potentially identify individuals at increased injury risk. Knowing the associations between individual anatomy and function can inform clinical decisions at the patient level, such as guiding tendon transfer surgeries and developing neuromuscular rehabilitation protocols.

Two limitations should be considered. First, results are limited to scapular plane

elevation. Second, we assumed the Z-axis of the modified scapular coordinate system, which differed from Ackland & Pandy (2009), aligned with the normal vector of the glenoid surface, which may not always be true. This could produce a systematic bias and may underestimate true between-subject variation, as we found that perturbing the scapular axes by ±15° altered rotator cuff stability ratios up to ±0.5 units.

In conclusion, this study determined the stability ratios of the scapulohumeral muscles, finding varying effects of muscle geometry on stabilizing functions. Inter-individual anatomical differences are expected to require altered muscular coordination. Future efforts should aim towards associating musculoskeletal geometry differences with muscle activity patterns throughout the shoulder range of motion, while accounting for altered scapular kinematics, in order to develop an integrated anatomical- and mechanics-based model determining the pathomechanics and risk for injuries.

Conflict of Interest Statement

The authors declare no conflicts of interest related to the manuscript.

Acknowledgements

This work was supported by research funding from the Natural Sciences and Engineering Research Council of Canada (NSERC Discovery Grant RGPIN-2016-06460 to PJK), and an NSERC CGSM to DM.

References

Ackland, D. C., Pak, P., Richardson, M., Pandy, M. G. 2008. Moment arms of the muscles crossing the anatomical shoulder. Journal of Anatomy, 213(4), 383-390.

Ackland, D. C., Pandy, M. G. 2009. Lines of action and stabilizing potential of the shoulder musculature. Journal of Anatomy, 215(2), 184–197.

Ameln, D., Chadwick, E., Blana, D., Murgia, A. 2018. The stabilizing function of superficial shoulder muscles changes between single-plane elevation and reaching tasks. IEEE Transactions on Biomedical Engineering, 66(2), 564-672.

Banas, M. P., Miller, R. J., Totterman, S. 1995. Relationship between the lateral acromion angle and rotator cuff disease. Journal of Shoulder and Elbow Surgery, 4(6), 454–461.

Bey, M. J., Kline, S. K., Zauel, R., Lock, T. R., Kolowich, P. A. 2008. Measuring dynamic in-vivo glenohumeral joint kinematics: technique and preliminary results. Journal of Biomechanics, 41(3), 711–714.

Blana, D., Hincapie, J. G., Chadwick, E. K., Kirsch, R. F. 2008. A musculoskeletal model of the upper extremity for use in the development of neuroprosthetic systems. Journal of Biomechanics, 41(8), 1714–1721.

Boileau, P., Walch, G. 1997. The three-dimensional geometry of the proximal humerus: implications for surgical technique and prosthetic design. The Journal of Bone and Joint Surgery, 79(5), 857–865.

Chopp, J. N., O'Neill, J. M., Hurley, K., Dickerson, C. R. 2010. Superior humeral head migration occurs after a protocol designed to fatigue the rotator cuff: A radiographic analysis. Journal of Shoulder and Elbow Surgery, 19(8), 1137–1144.

Chopp-Hurley, J. N., O'Neill, J. M., Dickerson, C. R. 2016. Distribution of bone and tissue morphological properties related to subacromial space geometry in a young, healthy male population. Surgical and Radiologic Anatomy, 38(1), 135–146.

Gerber, C., Snedeker, J. G., Baumgartner, D., Viehöfer, A. F. 2014. Supraspinatus tendon load during abduction is dependent on the size of the critical shoulder angle: a biomechanical analysis. Journal of Orthopaedic Research, 32, 952-957.

Graichen, H., Englmeier, K. H., Reiser, M., Eckstein, F. 2001. An in vivo technique for determining 3D muscular moment arms in different joint positions and during muscular activation - application to the supraspinatus. Clinical Biomechanics, 16(5), 389–394.

Halder, A. M., Halder, C. G., Zhao, K. D., O'Driscoll, S. W., Morrey, B. F., An, K. N. 2001a. Dynamic inferior stabilizers of the shoulder joint. Clinical Biomechanics, 16(2), 138–143.

Halder, A. M., Kuhl, S. G., Zobitz, M. E., Larson, D., An, K. N. 2001b. Effects of the glenoid labrum and glenohumeral abduction on stability of the shoulder joint through concavity-compression: an in vitro study. Journal of Bone and Joint Surgery - Series A, 83(7), 1062–1069.

Högfors, C., Sioholmt, G., Herberts, P. 1987. Biomechanical model of the human shoulder – I. Elements. Journal of Biomechanics, 20(2), 157–166.

Hughes, R. E., Bryant, C. R., Hall, J. M., Wening, J., Huston, L. J., Kuhn, J. E., Carpenter, J. E., Blasier, R. B. 2003. Glenoid inclination is associated with full-thickness rotator cuff tears. Clinical Orthopaedics and Related Research, 408(407), 86–91.

Kim, S. Y., Ko, J. B., Dickerson, C. R., Collins, D. F. 2017. Electromyographic investigation of anterior and posterior regions of supraspinatus: a novel approach based on anatomical insights. International Biomechanics, 4(2), 60–67.

Lee, S., Kim, K., O'Driscoll, S. W., Morrey, B. F., An, K. N. 2000. Dynamic glenohumeral stability provided by the rotator cuff in the mid-range and end-range of motion. Journal of Bone and Joint Surgery, 82–A(6), 849–857.

Lee, S., An, K. N. 2002. Dynamic glenohumeral stability provided by the three heads of the deltoid muscle. Clinical Orthopaedics and Related Research, 400, 40–47.

Lippitt, S., Matsen, F. 1993. Mechanisms of glenohumeral joint stability. Clinical Orthopaedics and Related Research, 291, 20–28.

Ludewig, P. M., Phadke, V., Braman, J. P., Hassett, D. R., Cieminski, C. J., Laprade, R. F. 2009. Motion of the shoulder complex during multiplanar humeral elevation. Journal of Bone and Joint Surgery - Series A, 91(2), 378–389.

Ludewig, P. M., Cook, T. M. 2000. Alterations in shoulder kinematics and associated muscle activity in people with symptoms of shoulder impingement. Physical Therapy, 80(3), 276–291.

Michener, L. A., McClure, P. W., Karduna, A. R. 2003. Anatomical and biomechanical mechanisms of subacromial impingement syndrome. Clinical Biomechanics, 18(5), 369–379.

Moor, B. K., Kuster, R., Osterhoff, G., Baumgartner, D., Werner, C. M. L., Zumstein, M. A., Bouaicha, S. 2016. Inclination-dependent changes of the critical shoulder angle significantly influence superior glenohumeral joint stability. Clinical Biomechanics, 32, 268-273.

Mulla, D. M., Hodder, J. N., Maly, M. R., Lyons, J. L., Keir, P. J. 2019. Modeling the effects of musculoskeletal geometry on scapulohumeral muscle moment arms and lines of action. Computer Methods in Biomechanics and Biomedical Engineering, 22(16), 1311-1322.

Nyffeler, R. W., Werner, C. M. L., Sukthankar, A., Schmid, M. R., Gerber, C. 2006. Association of a large lateral extension of the acromion with rotator cuff tears. Journal of Bone & Joint Surgery, American Volume, 88(4), 800–805.

Peltz, C. D., Baumer, T. G., Mende, V., Ramo, N., Mehran, N., Moutzouros, V., Bey, M. J. 2015. Effect of arthroscopic stabilization on in vivo glenohumeral joint motion and clinical outcomes in patients with anterior instability. The American Journal of Sports Medicine, 43(11), 2800-2808.

Poppen, N., Walker, P. 1976. Normal and abnormal motion of the shoulder. The Journal of Bone & Joint Surgery, 58, 195–201.

Poppen, N., Walker, P. 1978. Forces at the glenohumeral joint in abduction. Clinical Orthopaedics and Related Research, (135), 165–170.

Soslowsky, L., Malicky, D. M., Blasier, R. B. 1997. Active and passive factors in interior glenohumeral stabilization: a biomechanical model. Journal of Shoulder and Elbow Surgery, 6, 371–379.

Steenbrink, F., de Groot, J. H., Veeger, H. E. J., van der Helm, F. C. T., Rozing, P. M. 2009. Glenohumeral stability in simulated rotator cuff tears. Journal of Biomechanics, 42, 1740-1745.

Thompson, W. O., Debski, R. E., Boardman, N. D., Taskiran, E., Warner, J. J. P., Fu, F. H., Woo, S. L. Y. 1996. A biomechanical analysis of rotator cuff deficiency in a cadaveric model. American Journal of Sports Medicine, 24(3), 286–292.

Veeger, H. E. J., van der Helm, F. C. T. 2007. Shoulder function: The perfect compromise between mobility and stability. Journal of Biomechanics, 40(10), 2119–2129.

Webb, J. D., Blemker, S. S., Delp, S. L. 2014. 3D finite element models of shoulder muscles for computing lines of actions and moment arms. Computer Methods in Biomechanics and Biomedical Engineering. 17(8), 829-837.

Wu, G., Van Der Helm, F. C. T., Veeger, H. E. J., Makhsous, M., Van Roy, P., Anglin, C., Nagels, S., Karduna, A. R., McQuade, K., Wang, X., Werner, F. W., Buchholz, B. 2005. ISB recommendation on definitions of joint coordinate systems of various joints for the reporting of human joint motion - Part II: Shoulder, elbow, wrist and hand. Journal of Biomechanics, 38(5), 981–992.

Yanagawa, T., Goodwin, C. J., Shelburne, K. B., Giphart, J. E., Torry, M. R., Pandy, M. G. 2008. Contributions of the individual muscles of the shoulder to glenohumeral joint stability during abduction. Journal of Biomechanical Engineering, 130(2), 21024.

Table 1: List of scapulohumeral muscle sub-regions and number of elements (i.e. lines of action distinguishing groups of distinct muscle fascicles) representing each muscle included in the model. A description is provided for all muscle sub-regions, which were guided by the divisions made by Ackland et al. (2008). The inferior subscapularis, anterior deltoid, and middle deltoid were further divided as the different elements compromising these muscles displayed considerably different vector components and thus, stability ratios (as observable in Figure 2). Perturbations in attachment locations were conducted based on the anatomical vector variations reported in Högfors et al. (1987). With the exception of the infraspinatus (superior/inferior sub-regions) and subscapularis (superior/middle/inferior sub-regions), the study by Högfors et al. (1987) did not group muscles into sub-regions. Thus, perturbations to attachment locations were performed identically to all elements of the same muscle (e.g. same perturbations to both the anterior and posterior supraspinatus), except for the infraspinatus and subscapularis, where different perturbations were made for their respective sub-regions.

Muscle sub-region	Description	Number of Elements
I. Infraspinatus	Infraspinatus – Inferior region	3
S. Infraspinatus	Infraspinatus – Superior region	3
A. Supraspinatus	Supraspinatus – Anterior region	2
P. Supraspinatus	Supraspinatus – Posterior region	2
S. Subscapularis	Subscapularis – Superior region	3
M. Subscapularis	Subscapularis – Middle region	3
I. Subscapularis (L)	Subscapularis – Inferior region (long fibres)	3
I. Subscapularis (S)	Subscapularis – Inferior region (short fibres)	2
Teres Minor	Whole muscle	3
Teres Major	Whole muscle	4
A. Deltoid (1)	Anterior Deltoid (lateral most clavicular attachment)	1
A. Deltoid (2)	Anterior Deltoid (medial clavicular attachments)	3
M. Deltoid (1)	Middle Deltoid (posterior acromion attachments)	4
M. Deltoid (2)	Middle Deltoid (anterior acromion attachments)	3
P. Deltoid	Posterior Deltoid (scapular spine attachments)	4
Coracobrachialis	Whole muscle	3

Table 2: Mean with 95% confidence intervals [95% CI] and ± 1 standard deviation for model-predicted muscle stability ratios averaged across scapular plane elevation and grouped by scapulohumeral muscle sub-region due to changes in muscle attachment location. Stability ratios are in the superior/inferior direction (ST_{S-I}) and anterior/posterior directions (ST_{A-P}). Positive values for ST_{S-I} (ST_{A-P}) indicate the muscle would impose a superior (anterior) shear force at the humerus. Please refer to Table 1 for a description of all muscle sub-regions.

Muscle sub-region	ST_{S-I}		ST_{A-P}	
	Mean [95% CI]	**SD**	**Mean [95% CI]**	**SD**
S. Infraspinatus	-0.30 [-0.77, 0.18]	0.24	0.16 [0.00, 0.32]	0.08
I. Infraspinatus	-0.77 [-1.06, -0.47]	0.15	0.27 [-0.01, 0.55]	0.14
A. Supraspinatus	0.06 [-0.12, 0.24]	0.09	0.25 [0.07, 0.42]	0.09
P. Supraspinatus	0.02 [-0.19, 0.23]	0.11	0.17 [-0.04, 0.38]	0.11
S. Subscapularis	-0.10 [-0.53, 0.34]	0.22	-0.17 [-0.46, 0.12]	0.15
M. Subscapularis	-0.80 [-1.12, -0.48]	0.16	-0.22 [-0.39, -0.06]	0.08
I. Subscapularis (L)	-1.11 [-1.35, -0.87]	0.12	-0.32 [-0.56, -0.08]	0.12
I. Subscapularis (S)	-0.37 [-0.72, -0.03]	0.18	-0.48 [-0.75, -0.21]	0.14
Teres Minor	-0.63 [-1.01, -0.26]	0.19	0.29 [0.03, 0.56]	0.13
Teres Major	-0.43 [-0.67, -0.19]	0.12	-0.17 [-0.27, -0.08]	0.05
A. Deltoid (1)	1.01 [0.72, 1.30]	0.15	0.00 [-0.16, 0.15]	0.08
A. Deltoid (2)	1.14 [0.93, 1.35]	0.11	0.23 [0.12, 0.34]	0.06
M. Deltoid (1)	1.11 [0.90, 1.32]	0.11	-0.37 [-0.50, -0.24]	0.07
M. Deltoid (2)	1.00 [0.55, 1.45]	0.23	-0.29 [-0.62, 0.05]	0.17
P. Deltoid	0.66 [0.32, 1.01]	0.17	-0.20 [-0.50, 0.10]	0.15

Table 3: Regression models predicting muscle superior/inferior stability ratios (ST_{S-I}) at the glenohumeral joint for each scapulohumeral muscle sub-region. Independent variables include attachment changes at the scapula (S_x, S_y, S_z) and humerus (H_x, H_y, H_z) in each axis. For the anterior deltoid, the attachment locations were changed at the clavicle (C_x, C_y, C_z) (denoted with an asterisk*). All attachment changes were centered relative to the mean and divided by the standard deviation (i.e. a beta coefficient of 0.1 is interpreted as a 1 standard deviation change in the independent variable predicts a 0.1 unit change in the dependent variable). Humeral elevation angle relative to the thorax (HT) and its quadratic (HT^2) terms were added as covariates. Values represent unstandardized beta coefficients. Positive superior/inferior stability ratios indicate the muscle would impose a superior shear force at the humerus. Note the poor model fit for the coracobrachialis as it exhibited exponential changes in stability ratios with alterations in attachment locations and elevation angle (denoted with a #). Separate regressions performed at HT elevation angles of 45°, 90°, and 120° lead to improved model fit for the coracobrachialis (see Table A.1 in the supplementary file).

Muscle	B_0	S_x or $*C_x$	S_y or $*C_y$	S_z or $*C_z$	H_x	H_y	H_z	HT	HT^2	R^2
S. Infraspinatus	-0.35	-0.01	0.23	-0.01	-0.02	-0.04	-0.01	6.85E-05	9.04E-06	0.99
I. Infraspinatus	-0.75	-0.02	0.23	-0.16	-0.03	-0.07	0.00	-1.61E-03	1.62E-05	0.95
A. Supraspinatus	0.08	0.01	0.07	0.04	-0.03	-0.01	-0.01	-2.19E-03	2.27E-05	0.94
P. Supraspinatus	-0.07	0.00	0.10	0.03	-0.03	-0.01	-0.02	7.55E-04	6.25E-06	0.97
S. Subscapularis	-0.10	0.01	0.20	0.02	0.00	-0.01	0.00	-9.38E-04	1.19E-05	0.97
M. Subscapularis	-0.49	-0.01	0.18	-0.10	-0.02	-0.04	-0.02	-6.50E-03	2.30E-05	0.93
I. Subscapularis (L)	-0.87	-0.02	0.20	-0.17	-0.02	-0.05	0.00	-8.58E-04	-3.22E-05	0.90
I. Subscapularis (S)	-0.36	-0.03	0.12	0.00	-0.01	-0.08	0.00	1.78E-03	-2.37E-05	0.94
Teres Minor	-0.46	-0.01	0.22	-0.08	-0.01	-0.06	0.02	-3.30E-03	9.08E-06	0.96
Teres Major	-0.27	0.00	0.07	-0.02	-0.01	-0.11	0.00	-3.17E-04	-2.48E-05	0.98
A. Deltoid (1)*	2.06	0.04	0.11	-0.03	-0.01	-0.01	-0.04	-1.66E-02	1.36E-05	0.95
A. Deltoid (2)*	3.04	0.04	0.09	0.00	-0.02	0.00	-0.03	-3.91E-02	1.33E-04	0.99
M. Deltoid (1)	3.28	-0.01	0.03	0.09	-0.04	-0.02	-0.03	-4.88E-02	2.02E-04	0.97
M. Deltoid (2)	1.95	-0.01	0.13	-0.03	0.00	-0.01	-0.01	-1.57E-02	2.06E-05	0.80
P. Deltoid	1.55	0.02	0.01	0.18	-0.02	-0.03	-0.02	-1.64E-02	3.90E-05	0.87
Coracobrachialis#	42.51	1.95	2.91	4.35	-1.52	-2.23	-0.59	-1.13E+00	6.91E-03	0.00

Table 4: Regression models predicting muscle anterior/posterior stability ratios (ST_{A-P}) at the glenohumeral joint for each scapulohumeral muscle sub-region. Independent variables include attachment changes at the scapula (S_x, S_y, S_z) and humerus (H_x, H_y, H_z) in each axis. For the anterior deltoid, the attachment locations were changed at the clavicle (C_x, C_y, C_z) (denoted with an asterisk*). All attachment changes were centered relative to the mean and divided by the standard deviation (i.e. a beta coefficient of 0.1 is interpreted as a 1 standard deviation change in the independent variable predicts a 0.1 unit change in the dependent variable). Humeral elevation angle relative to the thorax (HT) and its quadratic (HT^2) terms were added as covariates. Values represent unstandardized beta coefficients. Positive anterior/posterior stability ratios indicate the muscle would impose an anterior shear force at the humerus. Note the poor model fit for the coracobrachialis as it exhibited exponential changes in stability ratios with alterations in attachment locations and elevation angle (denoted with a #). Separate regressions performed at HT elevation angles of 45°, 90°, and 120° lead to improved model fit for the coracobrachialis (see Table A.2 in the supplementary file).

Muscle	B_0	S_x or *C_x	S_y or *C_y	S_z or *C_z	H_x	H_y	H_z	HT	HT^2	R^2
S. Infraspinatus	0.11	0.06	-0.02	-0.03	-0.03	0.01	0.03	9.62E-04	-2.06E-06	0.98
I. Infraspinatus	0.26	0.15	-0.03	-0.01	-0.03	0.02	0.04	-8.66E-05	2.02E-06	0.92
A. Supraspinatus	0.07	0.09	0.00	-0.02	-0.03	0.01	0.01	2.88E-03	-2.92E-06	0.96
P. Supraspinatus	0.08	0.09	-0.01	-0.03	-0.03	0.00	0.03	1.42E-03	-1.60E-06	0.98
S. Subscapularis	-0.17	0.07	0.01	-0.16	0.00	-0.01	0.00	3.48E-05	1.22E-06	0.95
M. Subscapularis	-0.31	0.04	0.01	-0.09	-0.03	0.01	0.01	4.13E-04	1.01E-05	0.92
I. Subscapularis (L)	-0.27	0.08	0.01	-0.14	-0.04	0.00	0.01	-1.96E-03	1.48E-05	0.92
I. Subscapularis (S)	-0.47	0.10	-0.02	-0.13	-0.07	0.00	0.03	2.53E-03	-3.26E-05	0.95
Teres Minor	0.18	0.08	0.03	-0.03	-0.02	0.02	0.11	2.25E-03	-7.65E-06	0.86
Teres Major	-0.12	0.03	0.00	-0.04	-0.01	0.00	0.01	-1.19E-03	5.79E-06	0.96
A. Deltoid (1)*	-0.51	0.03	0.04	-0.04	-0.01	0.02	0.03	1.45E-02	-8.51E-05	0.81
A. Deltoid (2)*	0.48	0.02	-0.01	-0.04	-0.01	0.03	0.01	-5.71E-03	2.44E-05	0.84
M. Deltoid (1)	-0.41	0.14	0.00	-0.09	-0.01	-0.01	0.01	1.74E-03	-1.41E-05	0.51
M. Deltoid (2)	0.26	-0.04	-0.06	0.05	-0.04	0.00	0.01	-1.36E-02	6.66E-05	0.89
P. Deltoid	-0.32	0.07	0.05	-0.14	0.01	0.01	0.02	2.67E-03	-1.06E-05	0.73
Coracobrachialis#	6.41	0.28	0.37	0.58	-0.30	-0.19	-0.07	-1.79E-01	1.10E-03	0.00

List of Figure Captions

Figure 1: Model-predicted muscle superior/inferior stability ratios (ST_{S-I}) acting at the humerus with varying attachment locations. All 1000 simulations are plotted as thin grey lines, with thick, dark coloured bands representing the median for each muscle sub-region (see exceptions for the pectoralis major, latissimus dorsi, and gravity plots below). Where multiple colours are used in a single plot, darker shades represent the superior sub-regions of the infraspinatus/subscapularis, anterior sub-region of the supraspinatus, and A. Deltoid (2) and M. Deltoid (2). For the pectoralis major (8 elements) and latissimus dorsi (6 elements), no attachment alterations were performed with the plotted values in thick grey representing the model's default condition for all elements comprising each muscle. The shear ratio component of the gravity (i.e. arm mass) is reported in the last plot Black lines represent experimental data reported by Ackland & Pandy (2009), which were calculated using a different scapular coordinate system (Z-vector calculated from TS-AC). Positive (negative) values indicate a muscle line of action exhibiting a superior (inferior) shear component. A value of 1.0 (unity) reflects a muscle with an equal vector component in the superior-inferior direction as compression.

Figure 2: Model-predicted muscle anterior/posterior stability ratios (ST_{A-P}) acting at the humerus with varying attachment locations. All 1000 simulations are plotted as thin grey lines, with thick, dark coloured bands representing the median for each muscle sub-region (see exceptions for the pectoralis major, latissimus dorsi, and gravity plots below). Where multiple colours are used in a single plot, darker shades represent the superior sub-regions of the infraspinatus/subscapularis, anterior sub-region of the supraspinatus, and A. Deltoid (2) and M. Deltoid (2). For the pectoralis major (8 elements) and latissimus dorsi (6 elements), no attachment alterations were performed with the plotted values in thick grey representing the model's default condition for all elements compromising each muscle. The shear ratio component of gravity (i.e. arm mass) is reported in the last plot. Black lines represent experimental data reported by Ackland & Pandy (2009), which were calculated using a different scapular coordinate system (Z-vector calculated from TS-AC). Positive (negative) values indicate a muscle line of action exhibiting an anterior (posterior) shear component. A value of 1.0 (unity) reflects a muscle with an equal vector component in the anterior-posterior direction as compression.

Figure 3: Scatterplot between model-predicted muscle anterior/posterior (ST_{A-P}) and superior/inferior (ST_{S-I}) stability ratios for each scapulohumeral muscle at four humeral elevation angles: (A) 30°, (B) 60°, (C) 90°, and (D) 120°. Symbols represent means with 2 standard deviation error bars in either direction. The dotted black asymmetrical ellipse represents experimental thresholds collected by Lippitt & Matsen (1993) (see discussion for details). As all muscle sub-regions are comprised of a number of muscle elements, there are multiple data points of the same colour to indicate elements within the same muscle sub-region. Note: the axes for subplot (A) are wider and do not show data for the coracobrachialis as it extended outside the range.

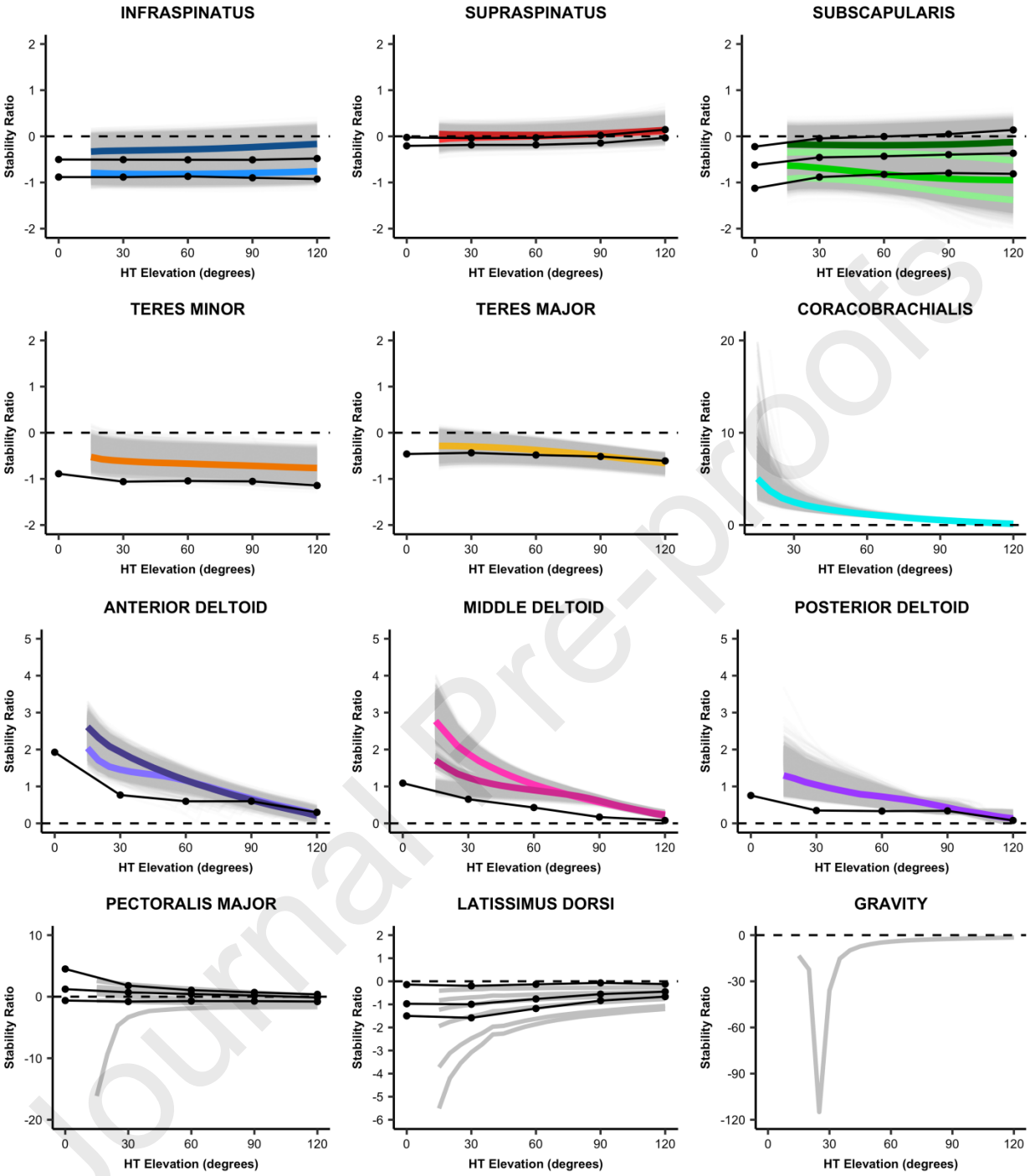

Figure 1

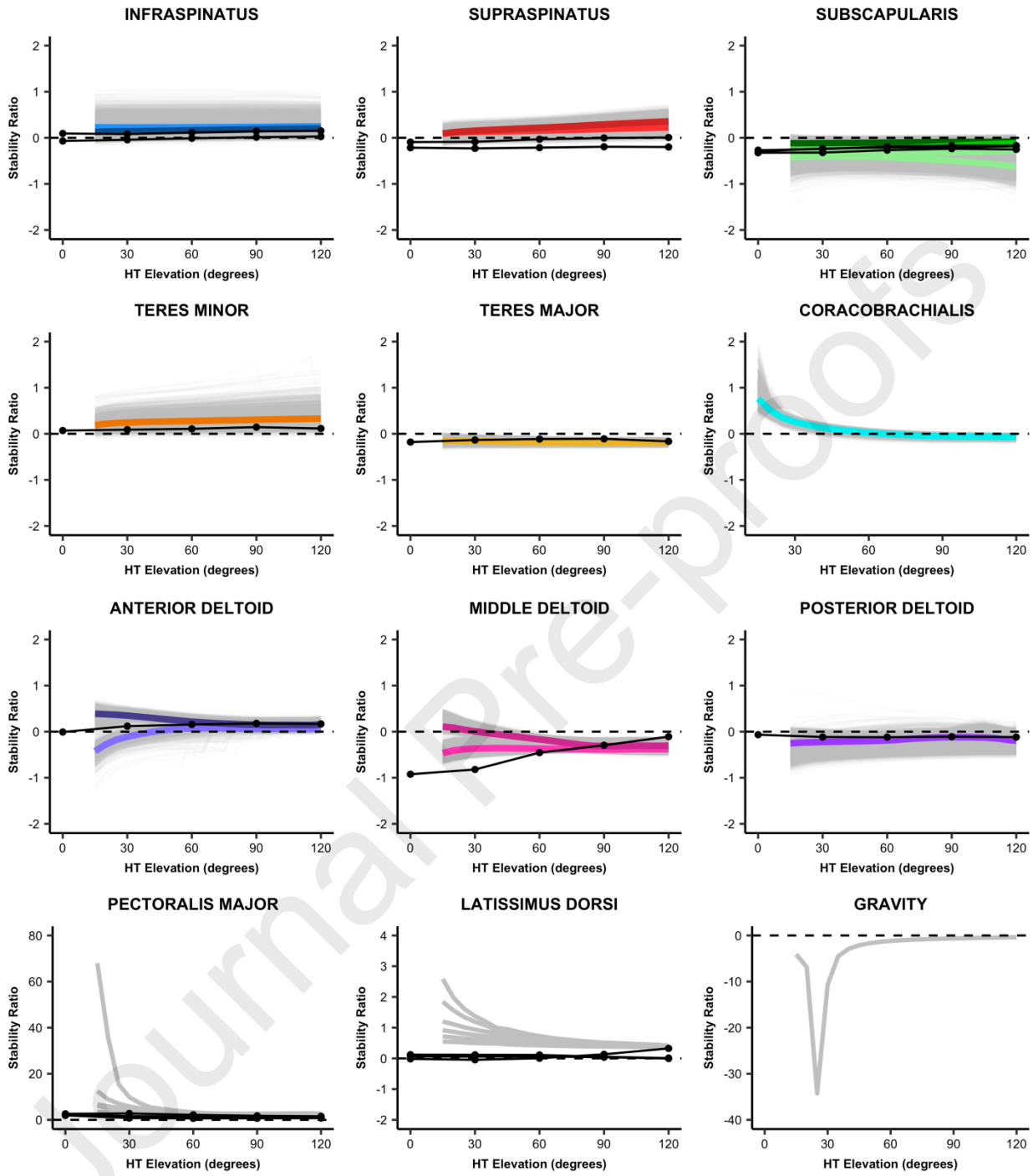

Figure 2

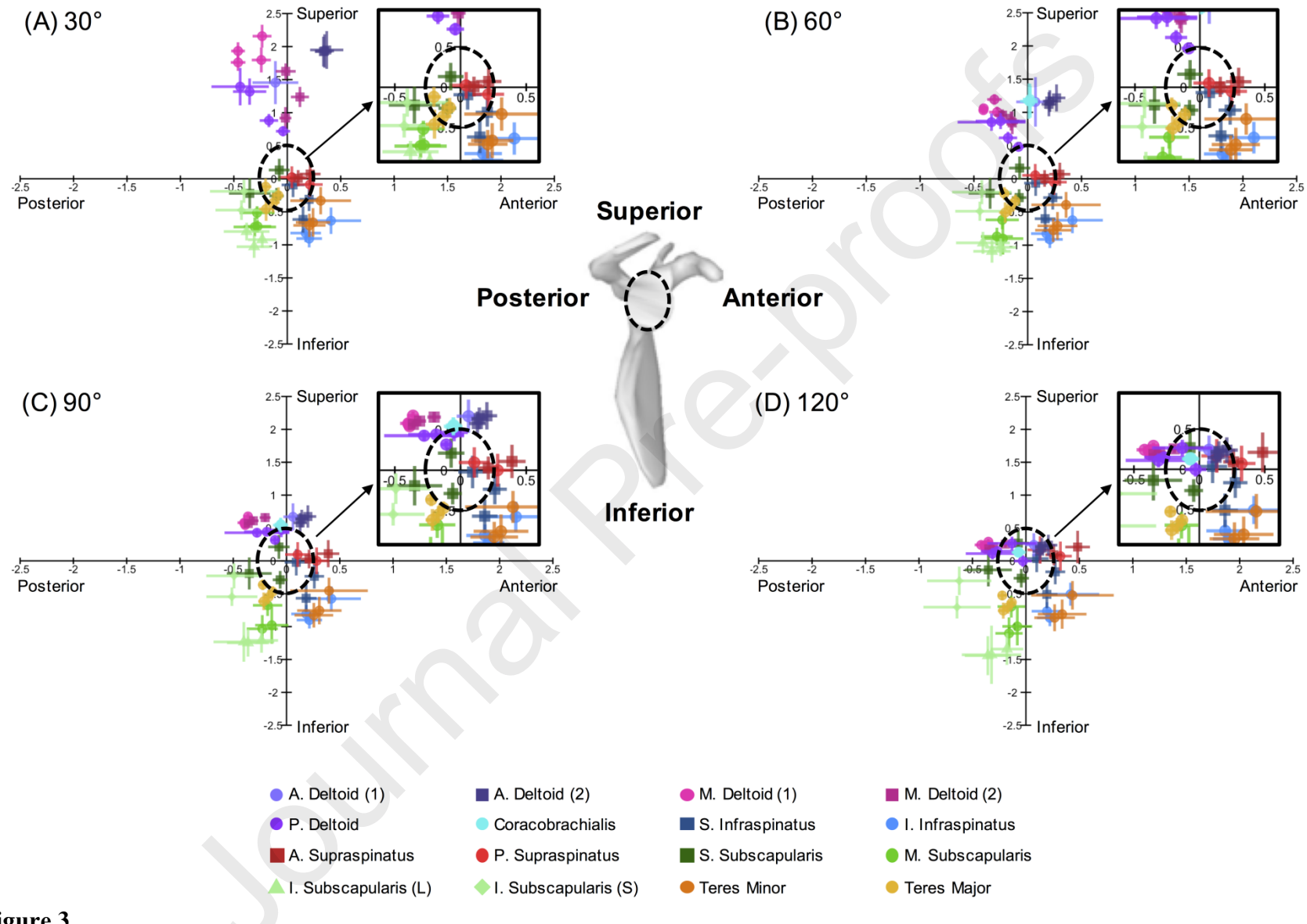

Figure 3